



Polarized emission from strongly magnetized sources

Roberto Taverna¹ , Roberto Turolla^{1,2}, Silvia Zane²,
Valery Suleimanov^{3,4,5}  and Alexander Y. Potekhin⁶

¹Department of Physics and Astronomy, University of Padova, via Marzolo 8, Padova, Italy
email: taverna@pd.infn.it

²Mullard Space Science Laboratory, University College London, Holmbury St. Mary, Surrey,
RH5 6NT, UK

³Institut für Astronomie und Astrophysik, Sand 1, D-72076 Tübingen, Germany

⁴Kazan (Volga region) Federal University, Kremlevskaja str., 18, Kazan 420008, Russia

⁵Space Research Institute of the Russian Academy of Sciences, Profsoyuznaya Str. 84/32,
Moscow 117997, Russia

⁶Ioffe Institute, Politekhnicheskaya 26, 194021, Saint Petersburg, Russia

Abstract. Anomalous X-ray pulsars (AXPs) and Soft gamma repeaters (SGRs) form together a single class of astrophysical sources, commonly associated to magnetars. New-generation X-ray polarimeters will play a key role in assessing the nature of these sources by directly probing the star magnetic field. In the highly magnetized environment radiation is expected to be strongly polarized and such a measure will be easily within reach of IXPE and eXTP. Polarization measurements will eventually confirm the presence of ultra-strong magnetic fields, probing the magnetar scenario. In this work we will discuss theoretical expectations for the polarization signature of AXPs and SGRs and present numerical simulations for the detector response of the polarimeters currently under construction. We will also show how these sources can be used to test vacuum birefringence, a QED effect predicted by Heisenberg and Euler in the Thirties and not experimentally verified as yet.

Keywords. stars: magnetars, polarization, techniques: polarimetric

1. Introduction

Magnetars form a particular group of isolated neutron stars (NSs) which are believed to host ultra-strong magnetic fields ($\approx 10^{14}$ – 10^{15} G), observationally identified with Anomalous X-ray Pulsars (AXPs) and Soft Gamma Repeaters (SGRs). They are characterized by a peculiar persistent X-ray emission, with luminosity (between $\approx 10^{33}$ and 10^{36} erg/s) typically in excess of the rotational energy-loss rate. In the soft X-ray band (0.5–10 keV), spectra are characterized by the superposition of two components, a thermal one, fitted by a blackbody (BB) with temperature typically around 0.5 keV, and a power-law tail at higher energies. Magnetars are also known for their bursting activity, which is for sure their most distinguishing observational manifestation, divided into short bursts, intermediate flares and giant flares, according to their duration and energy release (see [Mereghetti 2008](#) and [Turolla, Zane & Watts 2015](#) for reviews).

The theoretical model which most successfully explains magnetar phenomenology is the so-called twisted magnetosphere model ([Thompson, Lyutikov & Kulkarni 2012](#)). According to this, the internal magnetic field of magnetars is highly wound-up, with

a strong toroidal component able to exert a magnetic stress on the conductive surface. For magnetars, this toroidal component is strong enough to deform the crust, making the external magnetic field “twisted”. Such a configuration is not potential, so charged particles must flow along the closed field lines. The density of magnetospheric particles turns out to be high enough to make the medium in which thermal, surface-emitted photons propagate optically thick for resonant Compton scattering (RCS).

In the presence of ultra-strong magnetic fields, photons turn out to be linearly polarized in two normal modes, called ordinary (O) and extraordinary (X), with the photon electric field oscillating either in the $\mathbf{k}\mathbf{B}$ plane (with \mathbf{k} the photon wave vector and \mathbf{B} the local magnetic field direction) or perpendicularly to this plane, respectively. Photon polarization modes can change due to interactions with matter, like the magnetospheric charged particles which flow along the closed field lines. On the other hand, for B in excess of the quantum critical field $B_Q \simeq 4.4 \times 10^{13}$ G, quantum electrodynamics (QED) effects cannot be neglected, in particular vacuum birefringence (Heisenberg & Euler 1936), for which the virtual e^-e^+ pairs that populate the vacuum around the star are polarized by the strong NS field, modifying the dielectric and magnetic permeability tensors of the vacuum. It can be shown (Fernández & Davis 2011; Taverna et al. 2015) that, due to QED effects, photons propagating in the magnetized vacuum are forced to maintain their original polarization mode up to large distances from the source, making it possible to study the processes which occur at the surface through X-ray polarimetric observations.

X-ray polarimetry has attracted the interest of the scientific community particularly in the last months, with the successful launch of the new-generation X-ray polarimeter *IXPE* (Weisskopf et al. 2016) on December 9, 2021, which will be followed by the Chinese mission *eXTP* (Zhang et al. 2019) in 2027.

In this work we will present a numerical method to simulate the spectral and polarization properties of the persistent X-ray emission from magnetars within the RCS scenario, considering different models for photon emission from the surface. We show that polarization measurements may be indeed used to extract information on the physical and geometrical properties of the source, providing a tool to test for the first time the effects of vacuum birefringence.

2. Numerical implementation

For our simulations we used the Monte Carlo code originally developed by Nobili et al. (2008; see also Taverna et al. 2014). Although the twist of the external field is more likely localized into bundles of field lines, for the sake of simplicity we consider a globally-twisted dipole field. In this case the twist of the external field can be fully described by the twist angle,

$$\Delta\phi_{N-S} = \left[\frac{C(p)}{p(1+p)} \right]^{1/2} \lim_{\theta \rightarrow 0} \int_{\theta}^{\pi/2} \frac{f^{1/p}}{\sin \theta} d\theta, \quad (2.1)$$

where θ is the magnetic colatitude and the function f , the radial index p and the parameter C can be computed numerically (see Pavan et al. 2009 for more details). As a further simplification, we consider the charge carriers along the close field lines as electrons (unidirectional flow approximation, see Nobili et al. 2008). Under this assumption, the density of magnetospheric charges can be written as

$$n_e = \frac{p+1}{4\pi e} \left(\frac{B_\phi}{B_\theta} \right) \frac{B}{r|\langle\beta\rangle|}, \quad (2.2)$$

with e the electron charge and r the radial distance. We assume electrons distributed according to a 1D relativistic Maxwellian at the temperature $T_{e1} = 10$ keV, superimposed to a bulk motion at the velocity β (results do not depend much on the value of T_{e1}).

Photons are emitted from the star surface according to three different emission models (see Taverna *et al.* 2020 for further details). As a first-order approximation we consider photons following an isotropic BB at a constant temperature T over the surface. Since in strong magnetic fields the opacity for X-mode photons turn out to be strongly reduced with respect to that of O-mode ones (see e.g. Harding & Lai 2006), we assume in this case that photons are emitted 100% polarized in the X-mode. We then consider the case of radiation reprocessed in a geometrically-thin/optically-thick, pure-H atmospheric layer, properly accounting for the effects of strong magnetic fields on both spectra and polarization properties (Suleimanov *et al.* 2009). Finally, we contemplate the possibility that the star crust is composed by a magnetic condensate, which can be formed for sufficiently high magnetic field strengths and sufficiently low temperatures (see e.g. Turolla, Zane & Drake 2004; see also Potekhin 2014 for a review). In this case, emission is modeled in the free-ion and fixed-ion limits, both with proper spectral and polarimetric distributions (see Potekhin *et al.* 2012).

Once photons are launched from the surface (through a suitable acceptance-rejection method), they are followed during their propagation in the magnetosphere, accounting for both the effects of RCS and vacuum polarization. The latter are implemented by solving the wave equation in terms of the Stokes parameters I , Q , U and V . These are eventually summed together, once referred to the fixed polarimeter frame at infinity, providing spectra and polarization properties of the radiation at the observer for different viewing geometries and as functions of the star rotational phase.

3. Results

Using the code described in the previous section, we produced an archive of different simulations for the bright AXP 1RXS J170849.0–400910, each one labelled with different values of the twist angle $\Delta\phi_{N-S}$, the charge velocity β and the two angles χ and ξ which give the inclinations of the observer's line-of-sight and the star magnetic axis with respect to the star spin axis. For simplicity, we considered a homogeneous surface temperature $T = 0.5$ keV, which is representative for magnetar sources. Each simulation is performed twice, either considering (QED-ON) or neglecting (QED-OFF) vacuum polarization effects. In order to compare our numerical predictions with observations, we produced a 1 Ms *IXPE* simulated observation, starting from a specific simulation of the archive. Eventually, we fit the mock data obtained in this way with the entire archive of theoretical models, to recover the values of χ , ξ , $\Delta\phi_{N-S}$ and β and the emission model used for the simulated observation (as we will do for a real observation).

Figure 1 shows the mock data of the simulated *IXPE* measurement together with the best fitting theoretical curves. The left panel shows the phase-dependent polarization degree, energy-integrated in the 2–8 keV range (blue circles with error bars), with superimposed the best fitting QED-ON (orange-solid) and QED-OFF (orange-dashed) curves obtained using the BB emission model (which returned the best reduced chi-squared). As it can be clearly seen, QED-OFF simulations fail in reproducing the phase-dependent behavior of the polarization degree, providing, for all intents, an indirect proof of vacuum birefringence effects. The phase-integrated, energy-dependent Stokes parameters for the same simulated measurement are displayed in the right panel, with the solid curves marking the behaviors of I , Q and U again for the best fitting BB model QED-ON. We could check that all the other emission models (atmosphere and condensed surface) are excluded at a high level of confidence, confirming that polarimetry is indeed sensitive to the emission process which is at work at the surface. Finally, the input parameters we recovered joining together the results of the phase- and energy-dependent analyses do not differ much from the input ones (see Table 1), showing that polarization measurements will provide information on both the physical and geometrical properties of the source.

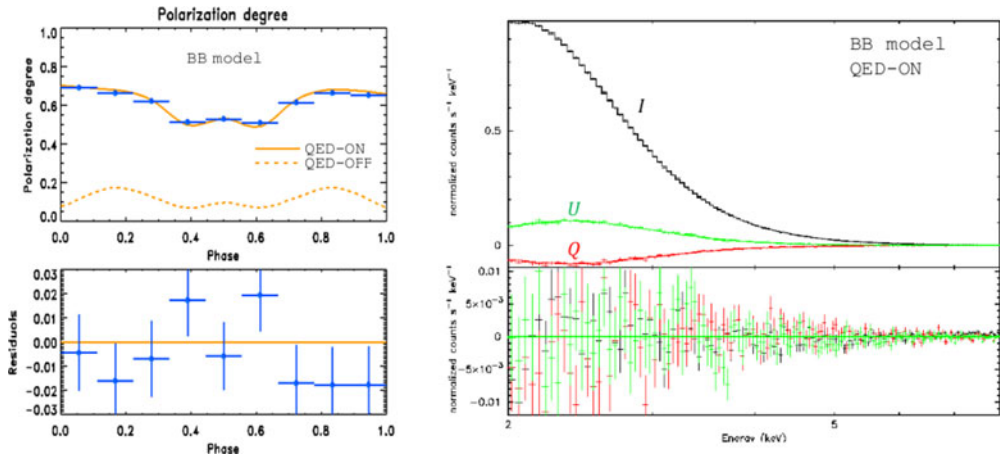


Figure 1. Best fit of the phase-dependent, energy-integrated polarization degree (left) and of the phase-integrated, energy-dependent Stokes parameters (right) obtained for a 1 Ms *IXPE* observation of the AXP 1RXS J170849.0–400910 (see text for further details).

Table 1. Best-fitting parameters obtained for the 1 Ms *IXPE* observation of the AXP 1RXS J170849.0–400910 displayed in Figure 1 (errors are given at 1σ).

| | Emission model | QED effects | χ ($^\circ$) | ξ ($^\circ$) | $\Delta\phi_{N-S}$ (rad) | β |
|----------|-------------------|-------------|---------------------|--------------------|--------------------------|-------------------|
| Input | BB 100%-polarized | QED-ON | 85 | 55 | 0.35 | 0.39 |
| Best fit | BB 100%-polarized | QED-ON | 82.68 ± 0.71 | 55.60 ± 0.41 | 0.300 ± 0.058 | 0.469 ± 0.008 |

References

- Fernández, R., & Davis, S.W. 2011, *ApJ*, 730, 131
Harding, A.K., & Lai, D. 2006, *Rep. Prog. Phys.*, 69, 2631
Heisenberg, W., & Euler, H. 1936, *Z. Phys.*, 98, 714
Mereghetti 2008, *A&AR*, 15, 225
Nobili, L., Turolla, R., & Zane, S. 2008, *MNRAS*, 386, 1527
Pavan, L., Turolla, R., Zane, S. & Nobili, L. 2009, *MNRAS*, 395, 1527
Potekhin, A.Y. 2014, *Phys. Usp.*, 57, 735
Potekhin, A.Y., Suleimanov, V., van Adelsberg M., & Werner K. 2012, *A&A*, 546, A121
Suleimanov, V., Potekhin, A.Y., & Werner K. 2009, *A&A*, 500, 891
Taverna, R., Muleri, F., Turolla, R., Soffitta, P., Fabiani, S., & Nobili, L. 2014, *MNRAS*, 438, 1686
Taverna, R., Turolla, R., González Caniulef, D., Zane, S., Muleri, F., & Soffitta, P. 2015, *MNRAS*, 454, 3254
Taverna, R., Turolla, R., Suleimanov, V., Potekhin, A.Y., & Zane, S. 2020, *MNRAS*, 492, 5057
Thompson, C., Lyutikov, M. & Kulkarni, S.R. 2002, *ApJ*, 574, 332
Turolla, R., Zane, S. & Drake, J.J. 2004, *ApJ*, 603, 265
Turolla, R., Zane, S. & Watts, A. 2015, *Rep. Prog. Phys.*, 78, 11
Weisskopf, M.C., et al. 2016, *Proc. SPIE Conf. Ser., Space Telescopes and Instrumentation, Ultraviolet to Gamma Ray. SPIE, Bellingham*, 9905, 990517
Zhang, S., et al. 2019, *Sci. China Phys. Mech. Astron.*, 62, 29502